UCRL-PROC-226274

LAWRENCE
LIVERMORE
NATIONAL
LABORATORY

Impedance Analysis of Electrochemical NOx Sensor Using a Au/Yttria-Stabilized Zirconia (YSZ)/Au cell

L. Y. Woo, L. P. Martin, R. S. Glass, R. J. Gorte

November 21, 2006

2006 MRS Fall Meeting
Boston, MA, United States
November 26, 2006 through December 1, 2006

Disclaimer

Impedance Analysis of Electrochemical NO_x Sensor Using a Au/Yttria-Stabilized Zirconia (YSZ)/Au cell

Leta Y. Woo[1,2], L. Peter Martin[1], Robert S. Glass[1], and Raymond J. Gorte[2]
[1]Energy and Environment Directorate, Lawrence Livermore National Laboratory, Livermore, CA, 94550
[2]Chemical and Biomolecular Engineering, University of Pennsylvania, Philadelphia, PA, 19104

ABSTRACT

An electrochemical cell employing a YSZ electrolyte and two Au electrodes was utilized as a model system for investigating the mechanisms responsible for impedancemetric NO_x (NO and NO_2) sensing. The cell consists of two dense Au electrodes on top of a porous/dense YSZ bilayer structure (with the additional porous layer present only under the Au electrodes). Both electrodes were co-located on the same side of the cell, resulting in an in-plane geometry for the current path. The porous YSZ appears to extend the triple phase boundary and allows for enhanced NO_x sensing performance, although the exact role of the porous layer is not completely understood. Impedance data were obtained over the frequency range of 0.1 Hz to 1 MHz, and over a range of oxygen (2 to 18.9%) and NO_x (10 to 100 ppm) concentrations, and temperatures (600 to 700°C). Data were fit with an equivalent circuit, and the values of the circuit elements were obtained for different concentrations and temperatures. Changes in a single low-frequency arc were found to correlate with concentration changes, and to be temperature dependent. In the absence of NO_x, the effect of O_2 on the low-frequency resistance could be described by a power law, and the temperature dependence described by a single apparent activation energy at all O_2 concentrations. When both O_2 and NO_x were present, however, the power law exponent varied as a function of both temperature and concentration, and the apparent activation energy also showed dual dependence. Adsorption mechanisms are discussed as possibilities for the rate-limiting steps.

INTRODUCTION

NO_x sensor development is motivated by environmental concerns and poses numerous challenges including cost, sensitivity, stability, and response time. Yttria-stabilized zirconia (YSZ) is currently used for automotive O_2 sensors and is particularly suited to meet the harsh, high-temperature operation requirements. Development of YSZ-based NO_x sensors has focused on amperometric and potentiometric types, usually relying on various metal-oxide electrodes to optimize the response [1-3]. Two major drawbacks have been device stability and the need for complicated structures to account for interfering gases, such as O_2. This paper presents an impedancemetric type YSZ-based model system, which has the possibility of overcoming problems associated with other types of sensors [4]. Previous work reported an impedancemetric NO_x sensor using Au, porous YSZ/Cr_2O_3 composite electrodes, and a YSZ electrolyte in an in-plane geometry [4]. Understanding the sensing mechanisms is necessary to optimize sensor operation. The present work uses a model electrochemical cell to isolate the role of the Au/porous YSZ interface. The cell consists of a dense YSZ electrolyte and two planar Au plates, with a porous YSZ layer separating the Au and dense YSZ. Impedance spectroscopy measurements were performed and then fit with an equivalent circuit. Data taken at different temperatures (600, 650, and 700°C) and concentrations are used to interpret the effect of O_2 (2, 10.5, 18.9%) and

NO_x(10, 50, 100 ppm). The analysis provides a basis for future work on the role of different oxides (e.g., Cr_2O_3), microstructures (e.g., porosity), and other material parameters.

EXPERIMENTAL DETAILS

YSZ powder (Tosoh 8-YS) was pressed and sintered at 1450°C producing dense 12.2 mm dia. pellets. YSZ powder dispersed in a 50% H_2O/50% ethanol solution was spray coated on the pellet as two side-by-side rectangles (each with area ~28 mm^2) separated by ~0.5 mm and fired at 1000°C. Figure 1a shows an SEM image of the ~10 μm thick porous YSZ layer consisting of ~100 nm dia. particles (Fig. 1b). Two Au plates contacted the porous YSZ using constant spring-loaded pressure. Testing occurred in a quartz tube (I.D. of 16.8 mm) inside a tube furnace with both electrodes exposed to the same gas (flow rate of 500 ml/min). Composition was controlled by mixing air, N_2, and 1000 ppm NO or NO_2 using thermal mass flow controllers. Electrochemical measurements were performed using a Solartron Analytical SI 1260 Impedance/gain-phase analyzer with the Solartron Analytical SI 1287 electrochemical interface and computer-controlled data acquisition with the commercially available ZPlot software (Scribner Associates, Inc.). Impedance spectra were collected from 1 MHz to 0.1 Hz at 20 steps per frequency decade with an excitation voltage of 50 mV and were subsequently analyzed using Boukamp's EQUIVCRT.COM software [5].

DISCUSSION

Figure 2a shows a Nyquist plot of the cell at 600°C in 2% O_2 with and without 100 ppm NO. A high-frequency (HF) arc, which does not change, is shown in the inset, while a larger low-frequency (LF) arc, which decreases significantly with the introduction of NO, dominates the spectra. The magnitude ($|Z|$) and phase angle (θ) at 10 Hz are graphically illustrated as solid and dotted lines, respectively, where $|Z|_1$ and θ_1 refer to the response in 2% O_2, and $|Z|_2$ and θ_2 refer to the response in 2% O_2 with 100 ppm NO. The response to NO_2 was qualitatively similar to that for NO. Miura, et al., and Wu, et al., have seen qualitatively similar response and utilized $|Z|$ as the sensing signal at 1 Hz and 0.42 Hz, respectively [6,7]. Figure 2 shows that θ may also be suitable for sensing. Previous work demonstrated that θ may be more sensitive than $|Z|$ at higher frequencies (~10 Hz) [4]. In general, higher frequency operation is desirable since it allows for reduced sampling times and potentially lower noise background [4]. The present work focuses on interpreting the response of the model electrochemical cell in the range of ~10 Hz to varying O_2 and NO_x concentrations.

Changes in gas concentration primarily affect the LF arc, which can be approximated

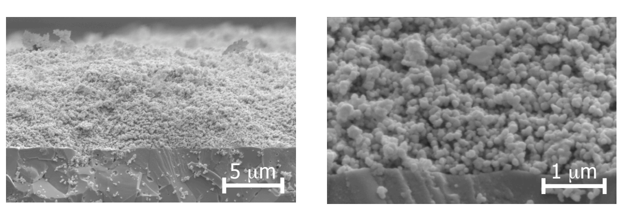

(a) (b)

Figure 1: SEM images of (a) the thickness and (b) morphology of the porous YSZ.

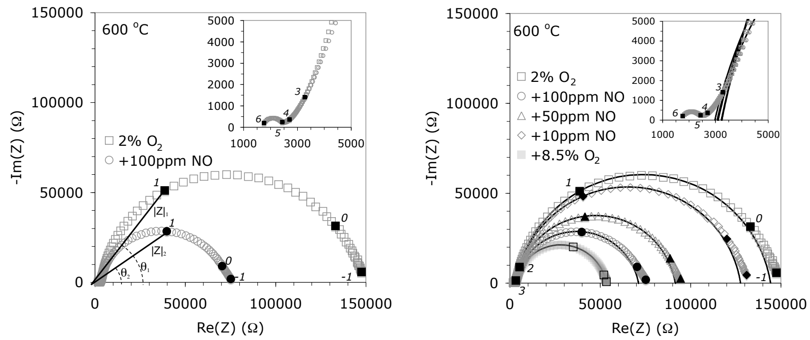

(a) (b)

Figure 2: Nyquist plot (darkened points are log frequency in Hz) showing (a) changes at 10 hz and (b) best-fit to the equivalent circuit (solid lines).

as a single arc using a simplified equivalent circuit consisting of a resistor (R_S) in series with a subcircuit made up of a resistor (R_{LF}) in parallel with a constant phase element (CPE). The CPE accounts for non-ideal behavior in real systems (i.e., “depressed” arcs in the Nyquist plot) and has the impedance relationship [8]: $Z(\omega) = [Y_0(j\omega)^{-n}]^{-1}$, where Y_0 is a constant, ω is angular frequency, and n is a measure of arc depression. For $n = 1$, there is no arc depression, and the impedance reduces to a capacitor with a value of Y_0. The experimental data were fit with the equivalent circuit using the partial non-linear least squares fitting routine in the Boukamp EQUIVCRT.COM software [5], and values for R_S, R_{LF}, and the CPE were obtained. R_S approximates the HF contribution to the total cell resistance, and R_{LF} corresponds to the diameter of the LF arc. The CPE n-values vary from $\sim$0.88 to $\sim$0.90, showing no temperature or concentration dependence. Since these n-values approach one, the best-fit values of Y_0 in the CPE are used as capacitance values.

Figure 2b shows Nyquist behavior with additions of NO; discrete points are experimental data, and solid lines are the best-fit using the equivalent circuit. There is good agreement between the fit and the measured data over the frequency range 1 Hz to 1 kHz. In Fig. 2b, adding either 8.5 % O_2 or 100 ppm NO produces similar decreases in the LF arc, $\sim$64% and $\sim$52%, respectively. This is remarkable since the NO concentration is $\sim 10^3$ times smaller than the O_2 concentration (i.e., 8.5%=85,000ppm). Additions of NO_x has a much larger effect on the electrical response than O_2. Calculated values of the circuit elements (i.e., the best-fit of the equivalent circuit to the experimentally measured data) for different gas concentrations and temperatures are used to determine possible rate-determining steps (RDS) and understand impedancemetric NO_x-sensing mechanisms.

The effect of O_2 on R_S and R_{LF} is shown in Fig. 3a, where R_S is insensitive to O_2. R_{LF} shows similar P_{O_2} dependences at all temperatures, with $R_{LF} \propto P_{O_2}^{-0.62}$. $R_{LF} \propto P_{O_2}^{-0.5}$ has been suggested for a RDS involving dissociative adsorption of O_2 [9, 10]. A surface diffusion process could also produce a similar dependence, but no limiting current behavior was observed. The deviation from -0.5 could result from the additional contributions of gas-phase diffusion or molecular adsorption, both of which have $R_{LF} \propto P_{O_2}^{-1}$ behavior [9]. An apparent activation energy (E_a) for R_{LF} of 98 kJ/mol for all O_2 concentrations is shown in Fig. 3b. Since R_S is insensitive to O_2, average values at all O_2 concentrations are

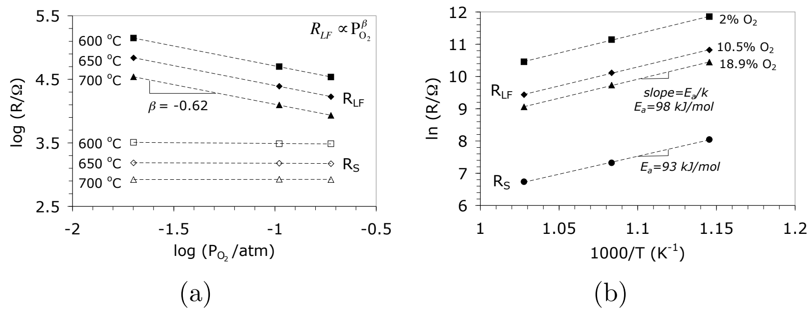

Figure 3: Variation of R_S and R_{LF} with (a) O_2 concentration and (b) temperature.

shown resulting in an E_a of 93 kJ/mol, which is consistent with ionic diffusion in YSZ. An E_a of 89 kJ/mole has been reported in a Au, O_2(g)/YSZ system [11]. Hertz, et al., found differing E_a for gold (88 kJ/mol) and platinum (74 kJ/mol) electrodes on thin film YSZ [12]. The similarity between these reported values and the present work may indicate that the response mechanism(s) are related to the Au/YSZ interface. The calculated capacitance exhibits only a slight dependence on temperature or O_2, in all cases ranging between 0.32 and 0.37 μF. However, general trends indicate that capacitance increases with P_{O_2}, which may be related to an increase in the fraction of adsorbed O_2 species at the Au/YSZ interface [11, 13].

The effect of NO_x on R_{LF} was qualitatively similar to the effect of O_2. R_S was insensitive to NO_x concentration. The NO_x dependence of R_{LF} (R_{LF/NO_x}) was determined by accounting for the effect of oxygen:

$$\frac{1}{R_{LF/NO_x}} = \frac{1}{R_{LF/O_2+NO_x}} - \frac{1}{R_{LF/O_2}} \tag{1}$$

where R_{LF/O_2+NO_x} is measured when both O_2 and NO_x are present, and R_{LF/O_2} is measured when only O_2 is present. Figure 4 shows that $R_{LF/NO_x} \propto [NO_x]^\alpha$, with $\alpha = -0.96 \pm 0.04$ and $\alpha = -1.02 \pm 0.16$ for NO and NO_2, respectively. R_{LF/NO_x} is effectively insensitive to P_{O_2} and shows very little sensitivity to temperature (see discussion below), so the average values are shown in Fig. 4 with error bars indicating the standard deviation. A possible explanation is a RDS controlled by molecular (non-dissociative) adsorption of NO and would be analogous to the molecular adsorption of O_2 which, when acting as the RDS, results in a power-law exponent of -1 [9]. In the current cell, dissociative adsorption of NO is not expected since it requires either an appropriate catalyst (e.g., Pt, Rh, and Pd) [14] or high electric fields [15, 16]; the absence of a limiting current suggests that gas phase diffusion is not the RDS. Thus, the NO_x dependence of R_{LF/NO_x} appears to be consistent with the non-dissociative adsorption of NO_x.

In general, the calculated E_a from R_{LF/NO_x} results in negative values for E_a, and R_{LF/NO_x} increases with temperature. This is in contrast to the behavior when only O_2 is present (see Fig. 3b), which has positive values of E_a and R_{LF} decreases with temperature. Increasing resistance with temperature has been attributed to adsorption processes, where the magnitude of E_a is related to the surface coverage [17]. For most values of NO_x, the calculated E_a from R_{LF/NO_x} range from -14 to -0.3 kJ/mol; the exception is 10 ppm NO_2,

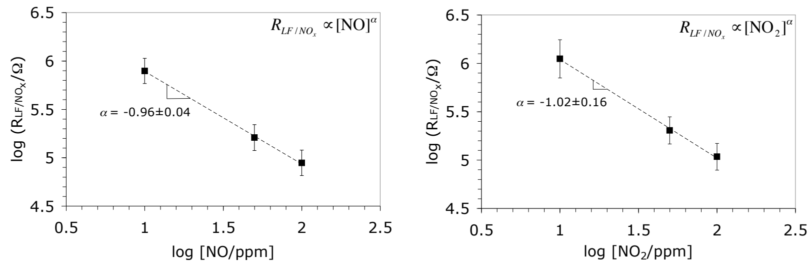

(a) (b)

Figure 4: NO_x concentration dependence for (a) NO and (b) NO_2.

which has larger magnitudes ranging from -54 to -34 kJ/mol. Nevertheless, in most cases, the calculated E_a values from R_{LF/NO_x} are significantly smaller in magnitude than the E_a calculated when only O_2 is present (98 kJ/mol). The differing magnitudes of E_a indicate that the effect of NO_x concentration on the LF arc is less sensitive to temperature than the effect of O_2. In general, the magnitude of E_a appears to decrease as NO_x concentration increases and O_2 concentration decreases. However, there is considerable scatter in the data. Although further studies are needed to explain the temperature dependence of R_{LF/NO_x}, the data seems to support a rate-limiting adsorption mechanism being responsible for the sensing behavior. The capacitance values for any combination of O_2 and NO_x concentrations at all temperatures tested were similar, with values ranging from 0.31 to 0.39 μF, and do not allow any definitive mechanistic conclusions.

When both NO_x and O_2 are present, the P_{O_2} dependence of the cell ($R_{LF/O_2+NO_x} \propto P_{O_2}^{\beta}$) varied with NO_x concentration and temperature. The absolute value of β decreases with additions of NO_x, an effect that becomes more pronounced at lower temperatures. The values of β range from -0.62 to -0.49, where the smallest absolute value of β occurs for 100 ppm NO at 600°C. The changing power-law exponent (β) could indicate changes in the RDS or the type of species involved [9]. When both O_2 and NO_x are present, E_a varies as a function of gas compositions, and is higher for the larger O_2 concentrations and always decreases with the addition of NO_x. The lowest E_a occurs for 2% O_2 and 100 ppm NO, with a value of 64 kJ/mol. Since adsorption processes appear to dominate the response, the decrease in E_a with the addition of NO_x may indicate changes in the adsorption energy and heat of adsorption. The trends could be interpreted as competition between the mechanisms responsible for the O_2 and NO_x responses, but are not completely clear at present.

CONCLUSIONS

Electrochemical characterization of a Au/YSZ/Au cell demonstrates that increases in either O_2 or NO_x concentrations decrease the LF arc diameter (R_{LF}), while HF behavior remains unaffected. Examination of the concentration and temperature dependences of R_{LF} provided mechanistic information. In the absence of NO_x, a single power-law exponent (-0.62) describes the P_{O_2} dependence (0.02 to 18.9 atm) of R_{LF} at all temperatures (600 to 700°C). Dissociative adsorption of oxygen is suggested as a possibility for the rate-determining step. Also, when only O_2 is present, a single E_a of 98 kJ/mol describes the temperature dependence for all concentrations, which may indicate the possible role of the Au/YSZ interface. The dependence of R_{LF/NO_x} on NO_x concentration (10 to 100 ppm) yields a power-law exponent of -1, and the molecular adsorption of NO is proposed as the RDS. When both O_2 and NO_x are present, the resulting E_a and P_{O_2} dependence vary with gas compositions and temperature, which may indicate competition between the two species. If adsorption processes are primarily responsible for the cell response, surface treatments of the YSZ could help to increase sensitivity and sensor signal. Further studies to elucidate the mechanisms are currently in progress.

ACKNOWLEDGEMENTS

This work was performed under the auspices of the U. S. Department of Energy by the University of California, Lawrence Livermore National Laboratory under Contract No. W-7405-Eng-48. Support for the work at the University of Pennsylvania was provided by the U.S. Department of Energy's Hydrogen Fuel Initiative (grant DE-FG02-05ER15721). Two of the coauthors (RSM and LPM) are also supported through the DOE Office of Freedom Car and Vehicle Technologies. We gratefully acknowledge the support of the Program Manager, Rogelio Sullivan.

REFERENCES

1. F. Ménil, V. Coillard, and C. Lucat, Sens. Actuators, B **67**, 1 (2000).
2. W. Göpel, G. Reinhardt, and M. Rösch, Solid State Ionics **136-137**, 519 (2000).
3. S. Akbar, P. Dutta, and C. Lee, Int. J. Appl. Ceram. Technol. **3**, 302 (2006).
4. L. Martin, L. Woo, and R. Glass, Submitted to J. Electrochem. Soc. (2006).
5. B. Boukamp, Equivalent circuit (equivcrt.pas), 1990.
6. N. Miura, M. Nakatou, and S. Zhuiykov, Sen. Actuators, B **93**, 221 (2003).
7. N. Wu, Z. Chen, J. Xu, M. Chyu, and S. Mao, Sens. Actuators, B **110**, 49 (2005).
8. J. Macdonald, *Impedance Spectroscopy: Emphasizing Solid Materials and Systems*, John Wiley and Sons, Inc., New York, 1987.
9. Y. Takeda, R. Kanno, M. Noda, Y. Tomida, and O. Yamamoto, J. Electrochem. Soc, **134**, 2656 (1987).
10. M. Koyama et al., J. Electrochem. Soc. **148**, A795 (2001).
11. B. van Hassel, B. Boukamp, and A. Burggraaf, Solid State Ionics **48**, 155 (1991).
12. J. Hertz and H. Tuller, J. Electroceramics **13**, 663 (2004).
13. T. Kenjo and K. Wada, Solid State Ionics **67**, 249 (1994).
14. D. Skelton, R. Tobin, D. Lambert, C. DiMaggio, and G. Fisher, Sens. Actuators, B **96**, 46 (2003).
15. S. Pancharatnam, R. Huggins, and D. Mason, J. Electrochem. Soc. **122**, 869 (1975).
16. H. Song, J. Moon, and H. Hwang, J. Eur. Ceram. Soc. **26**, 981 (2006).
17. O. Velle, T. Norby, and P. Kofstad, Solid State Ionics **47**, 161 (1991).